Ultra-Short Pulse Laser Ablation of Biological Hard Tissue and Biocompatibles

Martin STRASSL[*], Verena WIEGER[*], Daniel BRODOCEANU[§], Franziska BEER[#], Andreas MORITZ[#], and Ernst WINTNER[*]

[*]*Photonics Institute, Vienna University of Technology, Gusshausstrasse 27/387, 1040 Wien*
[§]*Institute of Applied Physics, Johannes Kepler University, Altenberger Str. 69, 4040 Linz*
[#]*Bernhard Gottlieb University Dental Clinic, Vienna Medical University, Währingerstr. 25a, 1090 Wien, Austria.*

E-mail: ernst.wintner@tuwien.ac.at

The application of ultra-short pulse lasers (USPLs) to biological hard tissue and compatible materials (like for dental restoration) in order to process cavities and more complicated structures is not yet a routine technique which can soon be implemented into practice. Its advantages, however, cover the feasibility of avoidance of collateral damage (i.e. thermal and shock wave), the creation of geometrically fully versatile and precise structures, and the option of spectroscopic feedback. In this paper, new data are presented concerning ablation rates and ablation thresholds of human and bovine dental hard tissue, dental composites and bone, i.e. compacta, spongiosa and cartilage, being ablated by various scanned USPLs with different pulse durations. The data give evidence that even ps pulses yield very useful results, and selective ablation may be beneficial for practical application. The morphology of the cavities yielded by different scanning techniques is analyzed via environmental scanning electron microscopy.

DOI: 10.2961/jlmn.2008.01.0007

Keywords: scanning of ultra-short laser pulses, dental cavity preparation, conservative dentistry, hard tissue processing, bone ablation, preparation quality, laser-induced break-down spectroscopy

1. Introduction

Ultra-short laser pulses (USLP) have been in the focus of interest for medical applications comprising diagnosis and tissue processing since more than 15 years. Many publications covered the mechanism of plasma-mediated ablation in general [e.g. 1-7], and the ablation of biological soft and hard tissues [e.g. 8-13] as well as the effects on the remaining structures [e.g. 14, 16]. Almost from the very beginning, special interest during these investigations was directed towards oral applications of ultra-short laser pulses, i.e. dentistry related applications [e.g. 8-11, 13-21]. This can be easily understood due to anatomic specialties like the shape of the tooth, for example, only allowing rather limited blood circulation, which accordingly does not allow efficient removal of externally applied heat. Hence it seems to be absolutely mandatory to process such tissue with only negligible heat and shock wave impact in order to also maintain the long-time vitality of a tooth [e.g. 10, 22, 23]. With conventional tools like mechanical dental drills or conventional dental laser systems (Er-based lasers), these requirements can be met only with strong efforts like e.g. intensive cooling by a water spray. However, the induction of micro-cracks in the tooth remains a rather unsolved problem (compare e.g. [17, 19, 24-27). Hence, from the beginning on the application of ultra-short laser pulses in dental hard tissue preparation was a very promising although rather complex approach. Some of the basic demands for successful hard tissue ablation by USLP, like spatial scanning of the beam, were very soon recognized and strictly demanded [e.g. 10, 19, 28].

After such insights, research throughout the last years moved towards the development of practically applicable systems [e.g. 16, 29, 30]. Even related findings like the ablation data of dental restorative materials or calcified plaque were reported for the first time. Corresponding publications e.g. can be found in [31, 32]. Also the preparation of bone and cartilage was resumed again, in oral treatments particularly under the aspect of keeping the processed surfaces biologically active for better tissue attachment to different implants [e.g. 33-36].

Beside the application of USLP, also development of commercial medical laser systems moved on towards more efficient systems for a broad variety of applications. By putting special attention on pulse durations, pulse energies and intensity distributions within the beam, the risks for hard

tissue treatment could be reduced [e.g. 34, 35] and thus the quality of prepared dentine cavities or cuts in bone increased. For these systems, however, the induced shockwaves and the need for cooling may still imply some limitation. Generally, the enormous costs far beyond 200 000 $ impose severe limitations for broad commercial development and applications.

2. Materials and Methods

2.1 Laser systems

Yb:Glass laser

Model IC1040-300 fs YB REG AMP (High Q Lasers), employed together with an x-y-scanner. Specifications: wavelength λ = 1040 nm, pulse duration τ_p = 330 fs, pulse repetition rate *PRR* = 0–10 kHz. Nevertheless, operation just at 1 kHz, thereby yielding the maximum average pulse energy E_{max} = 130 µJ; average power P_{ave} = 500 mW.

Ti:Sapphire laser

The Hurricane-i laser (Spectra-Physics) offers adjustable pulse duration τ_p = 130 fs – 7 ps. Specifications : $\lambda \approx$ 800 nm, E_p @ 1kHz ≥ 1 mJ, *PRR* = 0–10 kHz, but only 1 kHz used.

Table 1: Measured beam parameters of the Hurricane-i laser

	$2\omega_0$ [µm]	θ [rad]	ℓ_R [µm]	M^2
τ = 140 fs	67	0.025	1323	1.8
τ = 7 ps	70	0.026	1299	1.9

($2\omega_0$ beam waist, θ beam divergence, ℓ_R Rayleigh length, M^2 beam quality factor)

Nd:Vanadate Lasers:

Two USP Nd:Vanadate lasers (High Q Lasers) have been used. They belong to the so called "pico-REGEN^{TM} series", all-in-one picosecond regenerative amplifier systems. Both of these diode-pumped solid-state lasers have τ_p = 12 ps @ λ = 1064 nm, emitted with high temporal and spatial stability in a TEM_{00} mode (beam quality $M^2 \leq 1.2$). Differences between the two systems are with respect to P_{ave} = 1.5 W (IC-1500 REG AMP) vs. 10 W (IC-10000 REG AMP Microprocessing), *PPR* 0–5 vs. 0–100 kHz, E_p =300 µJ @ 5 kHz vs. 500 µJ @ 10 kHz, 200 µJ @ 50 kHz, and 80 µJ @ 100 kHz, respectively.

2.2 Samples

The samples comprised different dental hard tissues (human and bovine enamel and dentine), composite materials commonly used in dentistry (see Table 2) as well as bovine bone and cartilage tissue. The composites were prepared in form of cubes of 0.5 cm lateral width which were hardened by a light curing lamp. Dental and bone tissue has been cut into pieces of approximately 1×1×0.5 cm³. All the samples except bovine spongiosa and cartilage have been ground to smoothen the surface. Grinding of spongiosa and cartilage would have destroyed the natural morphology of the tissue. All the biological samples have been stored in water until the ablation.

The shape and tissues contained in a tooth can be assumed to be well-known. The bone compacta and spongiosa tissues are depicted for the example of human femur in Fig. 1.

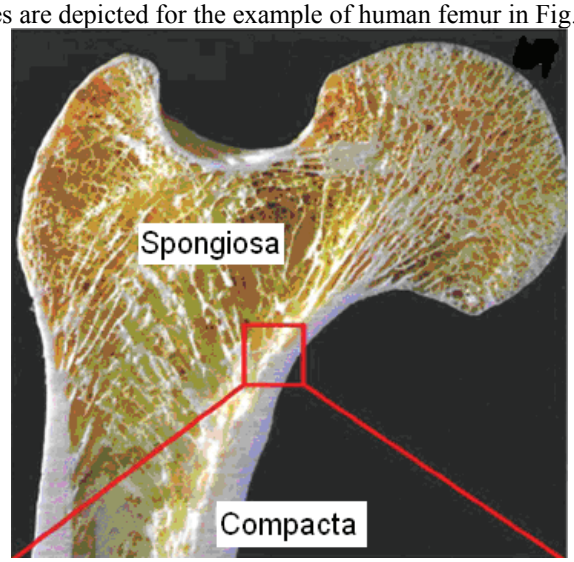

Fig. 1: Section through dried femur showing its internal architecture. Spongiosa with its trabecular meshwork can be distinguished from compact bone tissue. Pieces of bone like indicated have been used for the experiments.

Table 2: List of composites

Manufacturer	Product
Kerr Hawe	Point 4
	Premise Enamel
	Premise Body
	XRV Herculite Dentine
	XRV Herculite Enamel
Ivoclar Vivadent	Heliomar
	Compolgass F
	Tetric Flow
	Tetric Ceram
3M ESPE	Z100

Table 3: Specific densities and compositions of human and bovine spongiosa and compacta [38]

Bone tiss.	Orig.	Spec. dens. [gcm^{-3}]	Water fract. [vol%]	Miner. fract. [vol%]	Organ. fract. [vol%]	Anorg. fract. [vol%]
Spongiosa	Hum.	1.92	27.0	33.9	34.9	4.2
	Bov.	1.93	28.1	33.5	34.2	4.2
Compacta	Hum.	1.99	23.9	37.7	33.8	4.6
	Bov.	2.00	25.2	36.6	33.6	4.6

2.3 Evaluation

The USPL-treated samples were analyzed via digital light microscopy (Zeiss) as well as environmental scanning electron microscope (ESEM, see e.g. Fig. 3) in order to evaluate the ablation thresholds. Out of the micrographs, the diameters of the ablated shapes have been derived. To determine the threshold fluence of the materials, the diameters versus ener-

gies have been entered into an ln-plot. Regression tools and extrapolation allowed calculating the ablation threshold according to the following formalism:

$$\Phi(r) = \Phi_0 e^{-\frac{2r^2}{\omega_0^2}}, \quad (1)$$

where $\Phi(r)$ is the fluence at the radial distance r, Φ_0 the maximum fluence and ω_0 the radius of the beam waist. Assuming that a defined material dependent ablation threshold exists and that material surface perforation occurs when this threshold is exceeded, equation (1) can be rearranged to

$$r_{th}^2 = \frac{\omega_0^2}{2} \ln\left(\frac{\Phi_0}{\Phi_{th}}\right), \quad (2)$$

where r_{th} represents the radius of the ablation site at the ablation threshold Φ_{th}, implicating that at the rims of the damage zone the threshold fluence is reached. A logarithmic dependence on the ratio of the fluences Φ_0/Φ_{th} can also be stated for the etch depth per pulse d

$$d(\Phi) = \frac{1}{\alpha_{eff}} \cdot \ln\left(\frac{\Phi_0}{\Phi_{th}}\right), \quad (3)$$

wherein α_{eff} is the effective absorption coefficient. Fig. 2 demonstrates all these correlations (see [39] for all details).

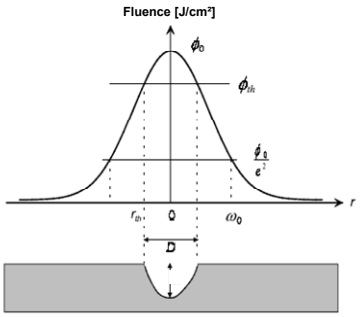

Fig. 2: Ablation with a Gaussian beam profile demonstrating the dependence of the damage radius r_{th} on the threshold fluence Φ_{th}. D is the diameter of the ablated cavity, d is the etch depth. (Figure taken from Bonse [37].)

2.4 Scanners

For the experiments requiring larger cavity sizes in order to demonstrate the morphology, two different scanners have been employed: a commercial x/y-scanner being best suited for the creation of rectangularly shaped as well as linear patterns, and a novel device following the geometry of r/φ coordinates. Thus, circularly shaped patterns easily could be achieved. In this r/φ-scanner (prototype developed by LINOS Photonics, Munich) used here, a conventional galvo-mirror deflecting the beam in radial direction and a fast picture rotating prism adding the φ-coordinate were implemented. By applying different motion functions and frequencies to the inclined mirror and specific rotation frequencies to the prism, various scanning patterns could be generated. In this way, cavities of conventional typical mm-size could be achieved.

After the experiments, the topography of the cavities was recorded and evaluated by modern digital light microscopy with implemented 3D reconstruction software (Infinite Focus Alicona Imaging, Grambach, Austria).

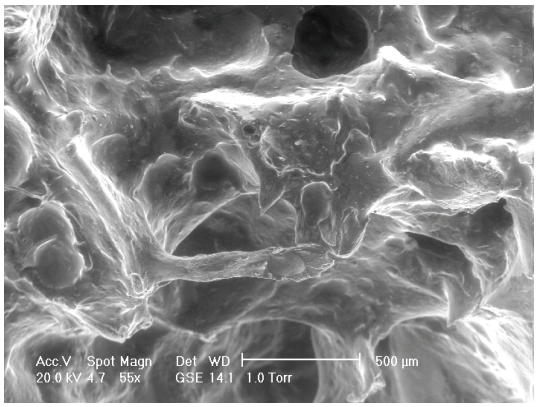

Fig. 3: ESEM micrograph of fresh human spongiosa. During storage the hard bone structure does not change, just fatty tissue and blood vessels dissolve.

3. Results

In general, within the limited space of this paper, just a selection of unpublished novel results yielded by USPL experiments are presented. Comparison is made with other results being published in [31, 32] or in the thesis [39].

3.1 Ablation rates of dental restoration material

Ablation rates (etch depth per pulse) were determined using either the 330 fs Yb:Glass laser or the Hurrican-i Ti: Sapphire laser with variable pulse duration. In this paper, 2 groups of results are shown: measurements on various composites carried out with the Yb:Glass versus fluence (Fig. 4) and similar measurements involving the Ti:Sapphire laser which in our setup allowed to choose between 4 different pulse durations (150 fs, 500 fs, 2 ps, 7 ps; Fig. 5). Thereby, line scans were conducted. The depths of the generated grooves were measured by means of digital light microscopy with implemented software. The primary motivation for these experiments is to allow an assessment of the removal capacity for dental restoration material in general, and in comparison with dental tissue in more detail (for which approximately ten times smaller ablation rates have been determined [39]) yielding quantitative data towards selective ablation as is also shown morphologically further down. Of course, linear fits would generate explicit values of threshold fluxes. It is, however, not aimed to enlist them here because of earlier publication [31]. Also α_{eff} could be derived easily if needed.

Concluding on the ablation rate measurements, it was shown that material removal by USPL can be very effective when certain laser parameters are applied and that ablation speeds comparable to Erbium systems can be achieved [39]. Moreover, the small ablation rates per pulse compared to Erbium systems ensure precise preparations without any

collateral damages. For minimal invasive dental treatments these properties are not enough. The potential of selective tissue processing is decisive, which is demonstrated below.

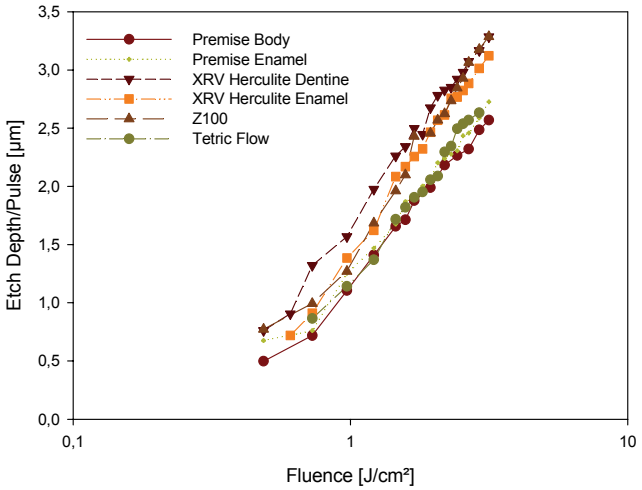

Fig. 4: Correlation between etch depth per pulse and laser fluence of the 330 fs Yb:Glass laser for dental restoration materials. Data are plotted in a semi-logarithmic plot to show the linear dependence.

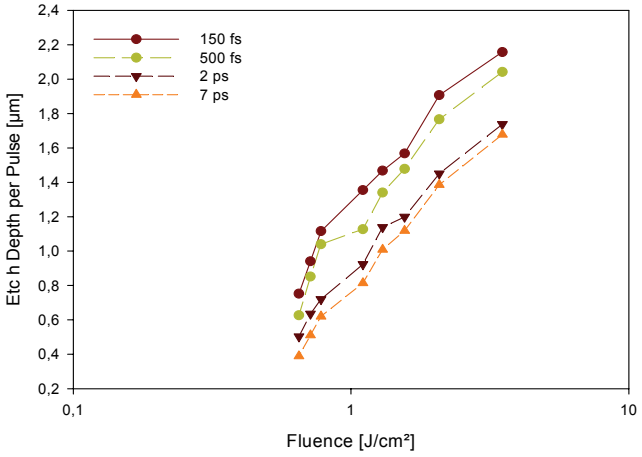

Fig. 5: Etch depth per pulse in Premise Enamel for rising pulse durations as an example, measured with the Ti:Sapphire laser.

3.2 Morphology of dental cavities

As dental drills are commonly used for cavity preparations, a micrograph of the remaining tissue morphology is provided in Fig. 6 and Fig. 7. The crack in Fig. 6 (right upper corner) arose from dehydration during ESEM investigation. Although the morphology of drilled cavities is often referred to as very smooth, the pictures below give another impression. Obviously, several steps in the cavity wall inclinations were unavoidable due to the shape of the drill. The surface is branded by the rotation of the drill visible as stripe-like traces. As expected the whole cavity is covered by a smear layer. Therefore, and this is well-known, an etchant has to be applied to open the tubuli and make them permeable for the primer to form tags for retention. Fig. 7 depicts the magnification of a cavity rim after etching with opened tubuli.

Fig. 8 represents a circular USLP-generated cavity by the r/φ-scanner on the dentine-Tetric Ceram border. To generate

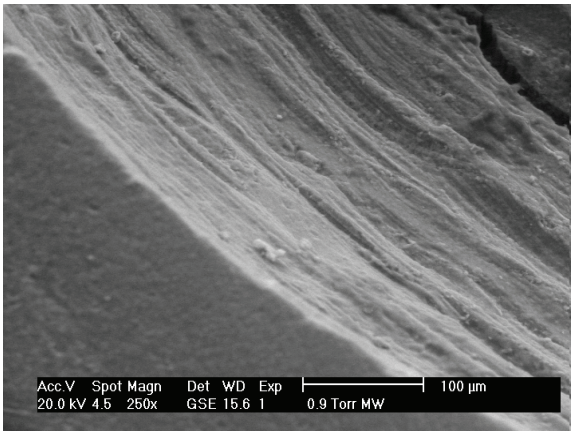

Fig. 6: Magnification of the cavity rim of a mechanically drilled cavity. The produced smear layer covers the dental tubuli.

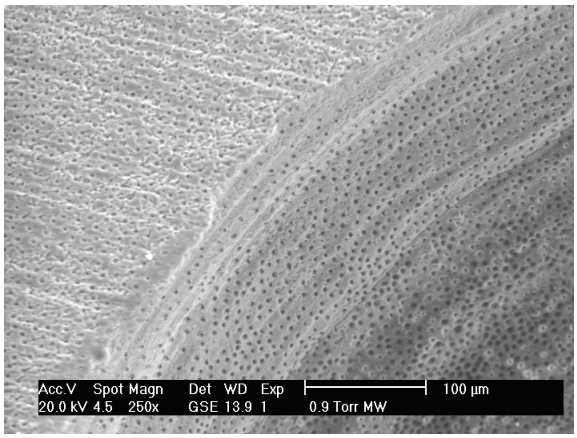

Fig. 7: Magnification of the rim of the cavity depicted above. After etching the dental tubuli are opened.

this cavity, laser treatment was performed for 2 minutes. The large cracks spreading over the whole cavity in Fig. 8a) are again due to dehydration during ESEM analysis. Concerning selectivity, the performance of the USPL is very impressive as a clear distinction between dentine and composite ablation sites can be made. In unison with the results of ablation rate measurements composite was removed on a much larger scale than dental tissue. Until now, selectivity was only judged on basis of SE micrographs.

As an additional tool, Infinite Focus light microscope analysis software was involved to provide another aspect of selective USPL ablation of composite and dentine. A three dimensional reconstruction of the generated cavity was obtained to give insight into the precipice created by composite ablation. This 3D cavity model is depicted in Fig. 8b).

The perfect micro-morphology of a small area inside a scanned cavity in dentine is to be seen in Fig. 9. The dentine tubuli are open without application of an etchant, and no traces of overheating leading to melting and re-solidification are observable.

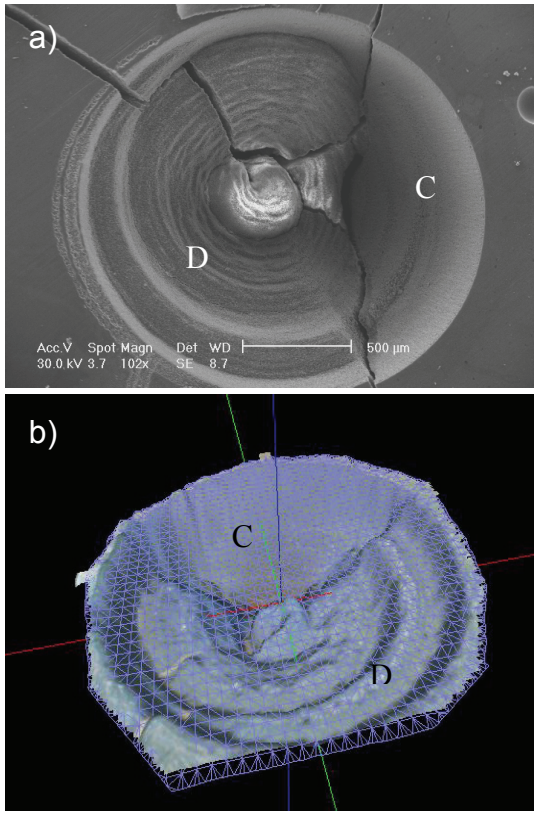

Fig. 8: a) ESEM of circularly scanned ablation crater obtained at the border between dentine (D) and composite (C) yielded by the 12 ps IC-1500 REG AMP Nd:Vanadate laser. b) 3D reconstruction of the same cavity by means of digital light microscopy using IFM.

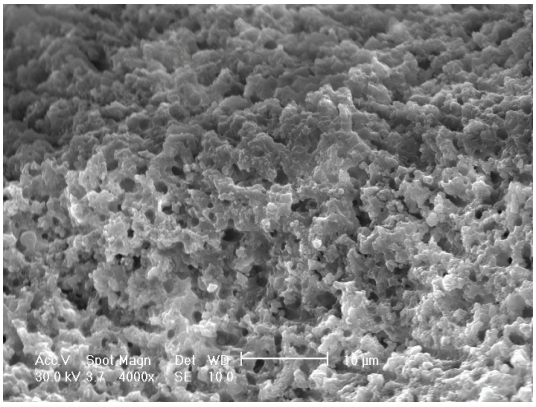

Fig. 9: ESEM of USPL-processed dentine revealing a perfectly maintained micro-structure with open tubuli and no trace of melting an re-solidification (12 ps Vanadate laser, E_p = 100 µJ) without any application of an etchant.

3.3 Ablation rates of bone tissues

Ablation rate measurements on compacta, spongiosa and cartilage tissues were carried out with pulse durations of

150 fs, 500 fs, 2 ps and 7 ps involving the Hurricae-i Ti:Sapphire laser, and with 330 fs generated by the Yb:Glass laser. A range of pulse energies E_p = 40 µJ – 240 µJ was covered and line scans were conducted. Again, the ablation rates, defined as etch depth per pulse, were calculated after determining the cavity depths and considering the equivalent pulse number. Fig. 10 shows the complete series of results.

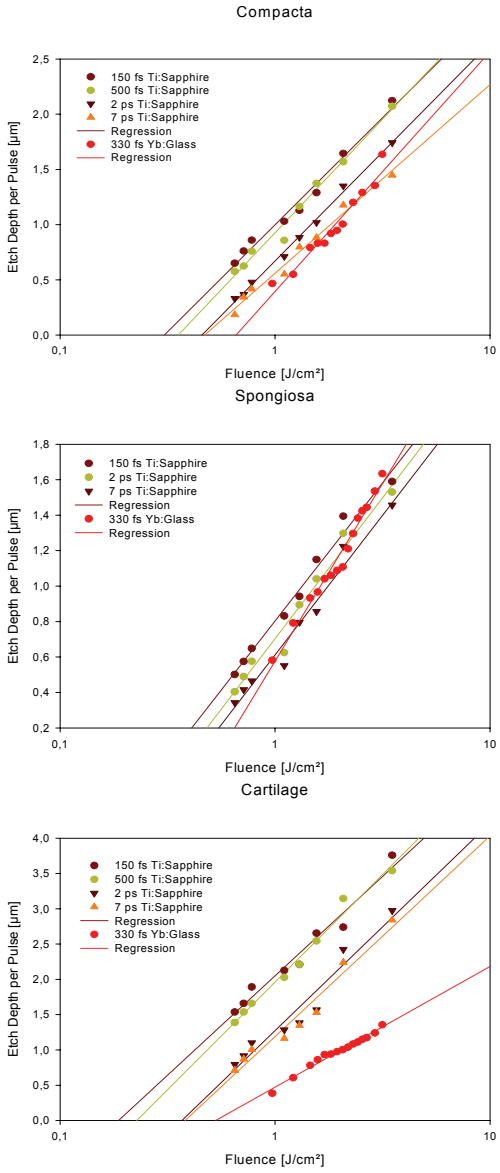

Fig. 10: Comparison of 150 fs – 7 ps Ti:Sapphire and 330 fs Yb:Glass laser ablation rates obtained in compacta, spongiosa and cartilage.

For every applied laser setting the etch depths per pulse for cartilage are the highest. 150 fs ablation revealed lower ablation rates for spongiosa compared to compacta, whereas spongiosa and compacta ablation rates are nearly the same for ps laser ablation. This finding is contrary to the one of Yb:Glass laser. Certainly, the reason therefore can be found in the native structure of spongiosa itself. As bone structure fits each individual's needs, differences can appear in the used samples. For some samples the bridge-like trabecula structure can be denser than for others, which means that the intra-trabecular space is smaller. A laser beam hitting the surface of denser spongy tissue removes material more efficient than the same laser beam impacting onto a coarser region. In the second case, there is no guarantee that each laser pulse strikes a trabeculum. Instead of that, the pulse may come down into the intra-trabecular space leaving the surrounding hard bone tissue untouched resulting in lower ablated depths. The obtained etch depths of spongiosa can therefore just serve as guidelines.

Alterations of the etch depths per pulse for varied pulse within 7 %. Further elongation of the pulse width induces a down scaling of 27 % and 17 %, respectively. Fig. 10 illustrates these facts.

The comparison of Yb:Glass and Ti:Sapphire laser ablation rates is still missing. Therefore, etch depths per pulse for all pulse durations of the Ti:Sapphire system as well as for 330 fs Yb:Glass laser ablation have been inserted into one plot for each bone material. Fig. 10 also demonstrates that spongiosa ablation rates of both systems cover almost the same range. Etch depths in compacta achieved by the 330 fs Yb:Glass laser integrate into the ps ablation rates of Ti:Sapphire. Just cartilage does not fit into the data range obtained by any Ti:Sapphire setting, but lacks behind.

3.4 Morphology of scanned cavities in bone tissues

The 330 fs Yb:Glass laser and the Ti:Sapphire laser with pulse durations of 700 fs and 7 ps were used for these studies. To prepare larger areas, the x-y-scanner was employed. Two scan patterns were programmed: A rectangular scan and an Archimedic spiral. The scan patterns were adjusted to the focal spot diameter and the *PRR* of the laser system, which means that the scan velocity and the distance between two traces of the scan pattern were chosen in order to yield a convenient overlap of subsequent laser pulses. When the overlap is too high accumulation effects influence the surface quality. The ablated cavities were investigated via ESEM.

When scanning the USPL beam according to an Archimedic spiral accumulation effects can be kept under control without the additional use of a shutter. The only issue is to select proper laser parameters. Fig. 11 comprises 700 fs Ti:Sapphire laser ablation of compacta with 0.65 J/cm² showing two different magnifications. The resulting cavity features including well-defined geometry, smooth cavity rims, the absence of debris and carbonisation are very appreciable. The natural structure of compacta was not affected either by the ablation. Cavity inclinations are clean and free of melting.

Fig. 12 alternatively (with respect to the laser system and to the scanning algorithm) shows rectangular scans of 330 fs Yb:Glass laser ablation of bovine spongiosa. It was ablated with 1.9 J/cm², which is more than twice the threshold value [39]. The overall view shows precise cavity geometry with defined and smooth edges. The natural structure of spongiosa

remained untouched without any carbonisation. Although no air-water-spray was used, no debris is evident. The magnification in Fig. 12b) captures the cut border of a trabeculum taken from the cavity edge. Compared to the cut borders generated by the mechanical drill or the Erbium system, the one presented here is very smooth. No micro-cracks or melting was introduced to the surrounding bone tissue. Looking at the edges of the rectangular cavity, melting caused by accumulation effects is visible. When the laser beam reaches the borders of the scan pattern it has to be shifted along a 90° line. After another 90° shift it moves its way back. Due to this turn an excessive number of laser pulses impacts onto the same tissue area. This effect is even more pronounced at the corners of the cavity. Nevertheless, by the implementation of a shutter this problem can easily be eliminated. Leaving the melting out of account, this is an excellent example of the non-destructive ablation procedure be USLPs.

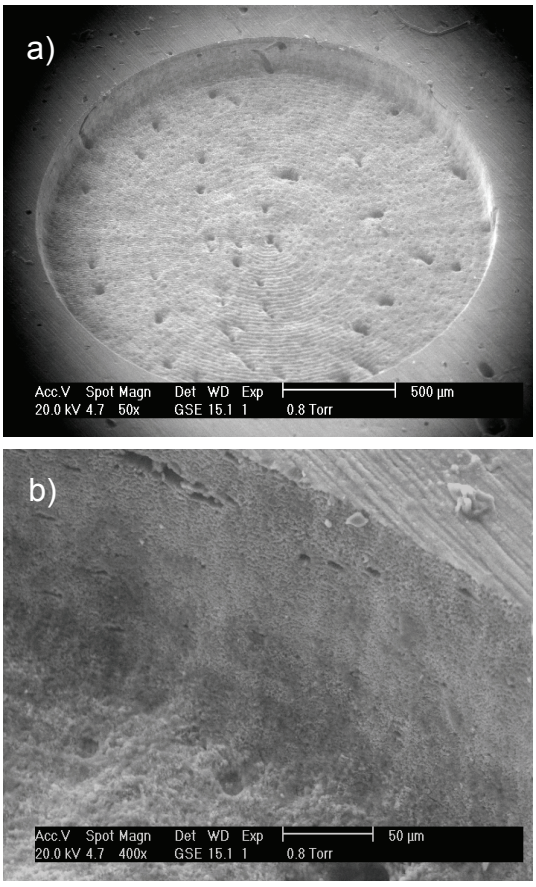

Fig. 11: Bovine compacta ablated by Ti:Sapphire laser pulses scanned according to an Archimedic spiral. Parameters: τ_p = 700 fs, *PRR* = 1 kHz, 20 roundtrips, Φ = 0.65 J/cm²; a) Overall view, b) magnification of the rim.

Although scanned USPL ablation of spongiosa has already been presented for the Yb:Glass system, pictures are also provided for the Ti:Sapphire ablation of the same tissue. As spongy tissue involved in the latter studies was strongly larded with fat, the appearance of the cavities after ablation is somewhat different. As evident in Fig. 13, bone got ablated properly, but a bubbled fat layer covers the whole cavity.

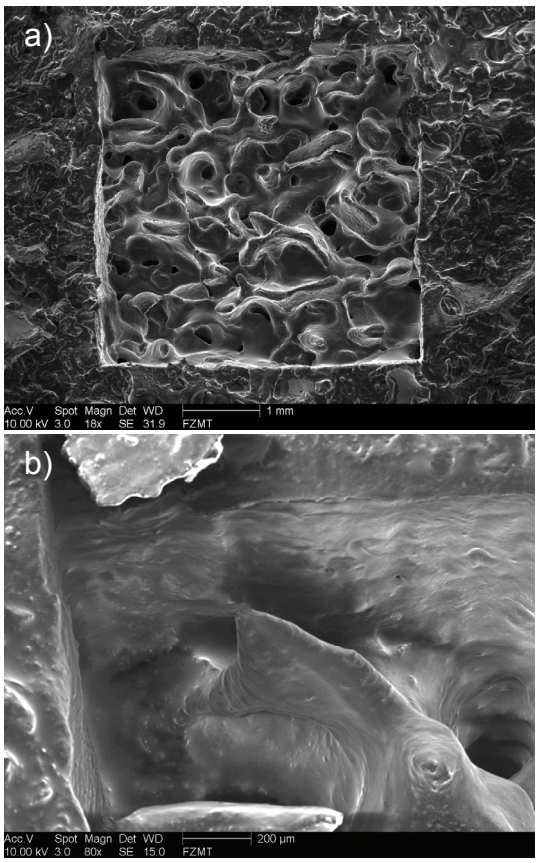

Fig. 12: Rectangular scan in bovine spongiosa ablated by the 330 fs Yb:Glass laser with Φ = 1.9 J/cm² and *PRR* = 1 kHz. a) Overall view of the cavity. b) Magnification of an edge of the cavity.

Anyhow, for the following healing process of bone no negative influences of this affected fat layer are expected. In praxis, cutting of cartilage might be more relevant than drilling circles as they are shown in Fig. 14. In both cases, the morphological features of the cut borders are expected to be of same satisfactory quality as reported here.

3.5 Laser-induced breakdown spectroscopy

For minimum invasive and selective treatment of different types of tissue a feedback system has to be established to reliably allow distinguishing between them. Laser-induced breakdown spectroscopy (LIBS) or sometimes referred to as laser-induced plasma spectroscopy (LIPS) as a non-contact in-situ method for elemental chemical analysis of the composition of substances, no matter if solid, liquid or gaseous, is therefore best suited.

When focusing a short high intensity laser pulse onto the surface of the sample of interest, free electrons are generated.

Subsequently, plasma is formed near the surface of the target by avalanche ionisation. This process is called optical breakdown. When the high density plasma expands into the ambient atmosphere the hot and radiating plasma plume cools down. The optical plasma emission is composed of transition

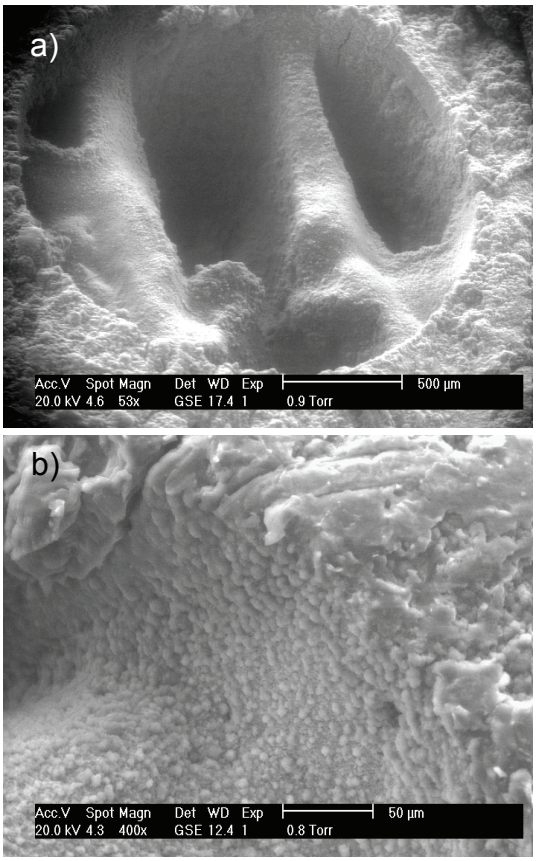

Fig. 13: Bovine spongiosa ablated by the Ti:Sapphire laser with additional circular scanning. Parameters: τ_p = 700 fs, Φ = 0.65 J/cm², *PRR* = 1 kHz, 20 roundtrips; a) Overall view of the cavity. b) Magnification of the cavity rim. The bubbles indicate fatty tissue.

lines of the material's constituents. By detecting these lines via a grating spectrometer information about the qualitative and quantitative composition of the target can be gained.
LIBS, which is applicable in a wide range of fields like material processing, space applications and also diagnostics, can be performed with ns, ps, and fs pulses. The latter are especially advantageous for analysis of biological samples with high spatial resolution [40]. Optical emission spectroscopy is just based on intrinsic light emission of the laser induced plasma. Therefore no other excitation source is needed. As a consequence, the experimental setup is quite simple and adaptable to automation and remote sensing. By that, even the temporal and spatial evolution of the plasma can be reproduced [41]. Performing LIBS nearly no sample preparation is necessary as laser ablation yields a fresh surface after each laser pulse. Spongiosa, compacta and cartilage, the targets of interest, were just cut to guarantee an even surface. The Hurricane-i Ti:Sapphire laser operated at a low *PRR* = 20 Hz was used for this studies. The plasma spark induced on the tissue surface was captured by a high resolution spectrometer, into which the light emitted from the plasma was coupled. This spectrometer contained a fiber combined with a time-resolved spectrally selective detector arrangement. All these units were computer controlled to ensure correct timing. The experimental setup is shown in Fig. 15.

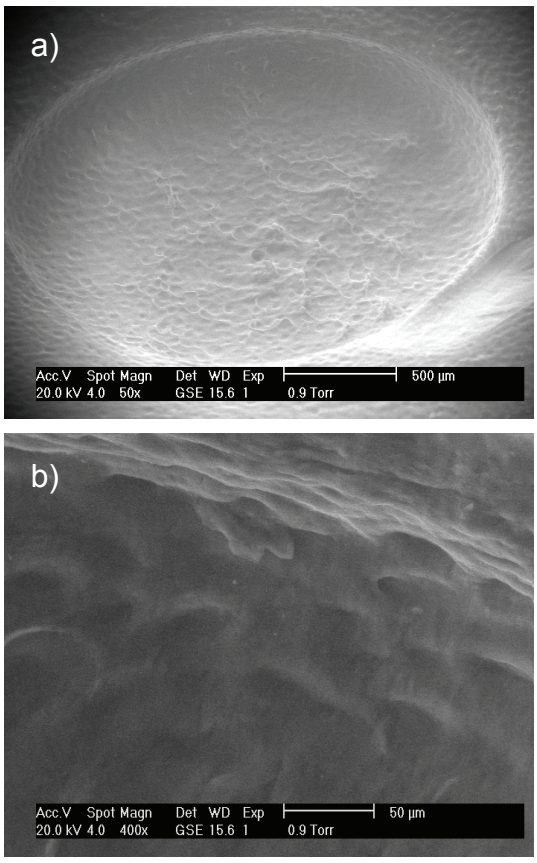

Fig. 14: Bovine cartilage ablated by the Ti:Sapphire laser following the traces of an Archimedic spiral. Parameters: τ_p = 700 fs, Φ = 0.65 J/cm², PRR = 1 kHz, 20 roundtrips; a) overall view, b) magnification of the crater rim.

Wavelength regions around λ = 422 ± 18 nm and λ = 526 ± 18 nm were investigated. Measurements were performed on three different spots on the tissue surface from where five spectra were taken. They were then averaged to eliminate inconsistencies. Peaks arising from the spectral continuum, which correspond to a transition from an upper to a lower excited level, were identified to be mainly Ca lines using the atomic spectra database of the National Institute of Standards and Technology [42].

As examples of the LIBS spectra acquired in this way for all types bone samples, spectra of λ = 422 nm are depicted in Fig. 16. The plots are normalized to their highest peak which can be ascribed to Ca. The height of the remaining peaks in

these plots gives their relative intensity in comparison to these Ca transition lines.

Besides a somewhat different appearance especially in the lower spectral range around 422 nm, cartilage can easily be distinguished from spongiosa and compacta by its generally lower ratios. Although the comparison between spongiosa and compacta affords a closer look, a distinction between those materials is also possible without a doubt. The ratios of the Ca peaks of 430.25 nm and 431.87 nm are ~18 % higher for compacta compared to spongiosa.

According to the results, plasma spectroscopy could be a valuable source to distinguish between different bone materials. A loop control system could be developed to automatically interrupt laser ablation when LIBS signalizes that biological tissue, that actually should be spared, was touched. A feedback system based on LIBS therefore could enhance selective and finally minimum invasive USPL treatment.

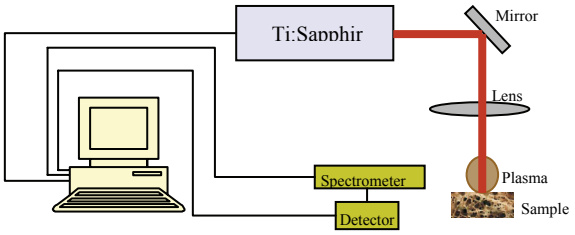

Fig. 15: Experimental setup for LIBS.

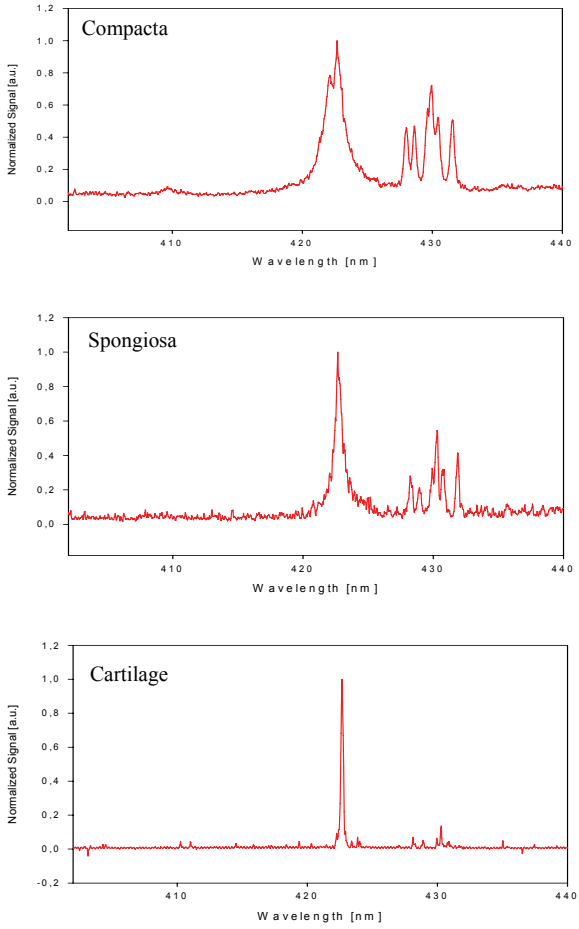

Fig. 16: LIBS spectra of spongiosa, compacta and cartilage depicting Ca peaks in the wavelength region of 422 ± 18 nm.

4 Summary and Outlook

The main results of this research work are summed up in the following (comparisons refer to data presented in detail in [39], which could not be shown in this concise paper):

- Etch depths per pulse achieved by USPL in dental hard tissue and composites are in the µm-region and hence much lower than Erbium laser ablation rates. USPL ablation can be enhanced by applying very high *PRR* > 10kHz. Ablation rates per second then become comparable to Erbium rates.
- Selective ablation is very pronounced for USPL as dentine revealed lower ablation rates than composites, being beneficial for minimum invasive secondary caries treatment.
- USPL thresholds of composites determined in this study are lower than those of tooth structures. Again, this fact contributes to selective ablation. With rising pulse duration thresholds increase and ablation rates decline at constant fluence.
- Scanned USPL ablation can provide a fine micro-retentive pattern. Although its appearance is distinct from an etched surface this regular structure bears the potential for good compound to dental filling material without additional etching.
- Like for tooth and composites, ablation rates per pulse achieved with Erbium lasers in bone material are generally higher than USPL ablation rates in the same tissue. Volumes in the order of 10^{-3}–10^{-2} mm³ per pulse can be excavated with Erbium lasers requiring fluences of tens of J/cm² while USPL are capable of just removing volumes in the order of 10^{-7} mm³ per pulse while applying about 2 J/cm² [39]. Consequently, for preparations within a reasonable duration high pulse repetition rates have to be used.
- Cartilage, the softest tissue, reveals the highest ablation rates, followed by compacta, the densest bone tissue. Spongiosa occupies the last position. This is a result of its native structure where laser pulses may hit an intratrabecular space and hence fail to contribute to ablation.
- The tissue morphology after preparation with a mechanical drill is characterised by torn out tissue particles and a smeared surface. USPL ablation of bone material was conducted with an x-y-scanner. In general, the native tissue structure was preserved. Although the gentle tissue removal procedure was demonstrated in spongiosa with 330 fs Yb:Glass laser at Φ = 1.9 J/cm² by performing rectangular scans, overheating and therefore melting can occur at the corners of rectangles. The beam of the Ti:Sapphire laser was scanned according to an spiral. For τ_p = 7 ps, *PRR* = 1 kHz, and Φ = 1 J/cm² acceptable results were achieved

[39]. For τ_p = 700 fs, *PRR* = 1 kHz, Φ = 1 J/cm² slight melting was evident. An improved match of scan and laser parameters is therefore inevitable. No morphological differences as well as no changes in the native structure could be detected for τ_p = 700 fs, Φ = 0.65 J/cm², and τ_p = 7 ps, Φ = 1 J/cm² ablation of cartilage at *PRR* = 1 kHz.

- During USPL ablation laser-induced plasma spectroscopy was performed. The relative intensities and widths of the identified Ca peaks potentially will allow differing between spongiosa, compacta and cartilage.

Considering all these aspects, superior ablation performance can be attributed to USPL systems in comparison to Erbium laser allowing positive expectations to future developments. A USPL system for surgical applications, e.g. implant surgery and orthopaedics, could be developed. A feedback system based on plasma spectroscopy to distinguish between different tissue types should be integrated. Furthermore, the scanner has to be miniaturized and incorporated into a handpiece to be operated by the surgeon. Such a USPL system can bring several advantages for the doctor as well as the patient, such as flexible, secure and gentle preparations, pain-free tooth treatment or, in case of bone, better healing conditions. Beside all such advantages, the prices for laser sources having the required specifications are still too high to allow the industrial development of a dental USP device for a broad market application at the moment. However, as USLP are in the state of entering broad-based industrial nowadays, the prices for adequate laser systems can be expected to go down within the next few years, thus giving new, positive perspectives to that problem.

Acknowledgements

Cordial thanks are expressed to J. Wernisch for his continuous support with his experience and ESEM micrographs. Support by High Q Lasers GmbH, Hohenems, Austria is acknowledged for providing access to their laser systems. Furthermore, we express our gratitude to Alicona Imaging GmbH, Grambach, Austria, for the possibility to perform 3D-cavity measurements in their labs. The work was partially funded by the Austrian Science Fund, Project P16133-N03.

References

1. B.C. Stuart, M.D. Feit, S. Hermann, A.M. Rubenchik, B.W. Shore, M.D. Perry: "Optical ablation by high-power short-pulse lasers", J. Opt. Soc. Am. B 13 (2), (1996) 459-468.
2. P. Gibbon, E. Förster: "Short-pulse laser-plasma interactions", Plasma Phys. Control. Fusion 38, (1996) 769-793.
3. M.H. Niemz: "Threshold dependence of laser-induced optical breakdown on pulse duration", Appl. Phys. Lett. 66 (10), (1995) 1181-1183.
4. M.D. Feit, A.M. Rubenchik, B.W. Shore: "Unique aspects of laser energy deposition in the fs pulse regime", SPIE 2672, (1996) 243-249.
5. B.C. Stuart, M.D. Feit, A.M. Rubenchik, B.W. Shore, M.D. Perry: "Laser-induced damage in dielectrics with nanosecond to subpicosecond pulses", Phys. Rev. Lett. 74 (12), (1996) 2248-2251.
6. T.V. Kononenko, V.I. Konov, S.V. Garnov, R. Danielus, A. Piskarskas, G. Tamoshauskas, F. Dausinger: "Comparative study of the ablation of materials by femtosecond and pico- or nanosecond laser pulses", Quant. Electron. 29 (8), (1999) 724-728.
7. B. Sallé, O. Gobert, P. Meynadier, M. Perdrix, G. Petite, A. Semerok: "Femtosecond and picosecond laser microablation: ablation efficiency and laser microplasma expansion", Appl. Phys. A 69, (1999) 381-383.
8. B.M. Kim, M.D. Feit, A.M. Rubenchik, D.M. Gold, B.C. Stuart, L.B. Da Silva: "Ultra-short pulse laser ablation of biological tissue", SPIE-BIOS'98, Jan. 24-30, (1998).
9. B.M. Kim, M.D. Feit, A.M. Rubenchik, E.J. Joslin, P.M. Celliers, J. Eichler, L.B. Da Silva: "Influence of pulse duration on ultra-short laser pulse ablation of biological tissue", J. Biomed. Opt. 6 (3), (2001) 332-338.
10. M.H. Niemz: "Laser-Tissue-Interactions: Fundamentals and Applications", Springer, Berlin 1996.
11. F.H. Loesel, M.H. Niemz, J.B. Bille, T. Juhasz: "Laser-induced optical breakdown on hard and soft tissues and its dependence on pulse duration: experiment and model", IEEE J. Quant. Electron. 32, (1996) 1717-1722.
12. A.A. Oraevsky, L.B. Da Silva, A.M. Rubenchik, M.D. Feit, M.E. Glinsky, M.D. Perry, B.M. Mammini, W. Small, B.C. Stuart: "Plasma-mediated ablation of biological tissues with nanosecond- to femtosecond laser pulses: relative role of linear and nonlinear absorption", IEEE J. Sel. Top. Quant. Electron. 2 (4), (1996) 801-809.
13. J. Neev, L.B. Da Silva, M.D. Feit, M.D. Perry, A. M. Rubenchik, B.C. Stuart: "Ultra short pulse lasers for hard tissue ablation", IEEE J. Sel. Top. Quant. Electron., 2(4), (1996) 790-800.
14. R.A. London, D.S. Bailey, D.A. Young, W.E. Alley, M.D. Feit, A.M. Rubenchik: "Hydrodynamic model for ultra-short pulse ablation of hard dental tissue", SPIE 2672, (1996) 231-242.
15. P.S. Banks, B.C. Stuart, A. Komashko, M.D. Feith, A.M. Rubenchik, M.D. Perry: "Femtosecond laser materials processing", SPIE 3934, (2000) 14-21.
16. J. Serbin, T. Bauer, C. Fallnich, A. Kasenbacher, W.H. Arnold: "Femtosecond lasers as a novel tool in dental surgery", Appl. Surf. Sci. 197-198, (2002) 737-740.
17. M.H. Niemz, L. Eisenmann, T. Pioch: "Vergleich von drei Lasersystemen zur Abtragung von Zahnschmelz", Schweiz. Monatsschr. Zahnmed. 103, (1993) 1252.
18. G.B. Altshuler, N.R. Belashenkov, V.B. Karasev, A.V. Skripnik, A.A. Solunin: "Application of ultra-short laser pulses in dentistry", SPIE 2080, (1993) 77-81.
19. A. Mindermann, M. Niemz, L. Eisenmann, F.H. Loesel, J.F. Bille: "Comparison of three different laser systems for application in dentistry", SPIE 2080, (1993) 68-76.
20. M.H. Niemz: „Schmerzfreie Zahnpräparation mit dem Nd:YLF-Pikosekundenlaser", Laser und Optoelektron. 26(4), (1994) 68-73.
21. A.A. Serafetinides, M. Khabbaz, M.I. Makropoulou, A.K. Kar: "Picosecond laser ablation of dentine in endodontics", Lasers Med. Sci. 14, (1999) 168-174.

22. L. Zack, G. Cohen: "Pulp response on external applied heat", OS, OM & OP 19 (4), (1965) 515-430.
23. K.M.Hargreaves, H.E. Goodis (Eds.): "Setzer and Bender's Dental Pulp", Quintessenz, Chicago, 2005.
24. R. Hibst: "Technik, Wirkungsweise und medizinische Anwendung von Holmium- und Erbium-Lasern", Habilitationsschrift, Ecomed, Landsberg 1996.
25. M. Frentzen, D. Hamrol: "Kavitätenpräparation mit dem Er:YAG-Laser - eine histologische Studie", Dtsch. Zahnärztl. Z. 55(2) (2000) 114-117.
26. K. Matsumoto, M. Hossain, N. Tsuzuki, Y. Yamada: "Morphological and Compositional Changes of Human Dentine after Er:YAG Laser Irradiation", JOLA 3(1) (2003) 15-20.
27. M. Hossain, J-I. Kinoshita, Y. Yamada, K.M. Rownak Jahan, Y. Nakamura, K. Matsumoto: "Compositional and Structural Changes of Human Dentine Following Er,Cr:YSGG Laser Irradiation In Vitro", JOLA 3(1) (2003) 23-28.
28. B.M. Kim, M.D. Feit, A.M. Rubenchik, L.B. Da Silva: "Medical applications of ultra-short pulse lasers", CLEO'99.
29. M. Strassl, A. Kasenbacher, E. Wintner: "Ultra-short laser pulses in dentistry", JOLA 2 (4), (2002) 213-222.
30. M.H. Niemz, A. Kasenbacher, M. Strassl, A. Bäcker, A. Beyertt, D. Nickel, A. Giesen: "Tooth ablation using a CPA-free thin disk femtosecond laser system", Appl. Phys. B 79 (3), (2004) 269-271.
31. V. Wieger, M. Strassl, E. Wintner: "Pico- and micro-second laser ablation of dental restorative materials", Laser and Particle Beams, 24, (2006) 41-45.
32. A. Yousif, M. Strassl, V. Wieger, S. Zoppel, E. Wintner: "Oral applications of ultra-short laser pulses – a new approach for gentle and painless treatment?", SPIE 6261, (2006), 626111.
33. H. Lubatschowski, A. Heisterkamp, F. Will, A.I. Singh, J. Serbin, A. Ostendorf, O. Kermani, R. Heermann, H. Welling, W. Ertmer: "Medical applications for ultrafast laser pulses", RIKEN Review 50, (2003) 113-118.
34. J. Neev, L.B. Da Silva, M.D. Feit, M.D. Perry, A.M. Rubenchik, B.C. Stuart: "Ultra-short pulse lasers for hard tissue ablation", IEEE J. Sel. Top. Quant. Electron. 2 (4), (1996) 790-800.
35. A. Kurella, N.B. Dahotre: "Surface modification for bioimplants: the role of laser surface engineering", J. Biomat. Appl. 20, (2005) 0885-3282/05/01 0005–46.
36. Y. Liua, S. Sunb, S. Singhaa, M.R. Chob, R.J. Gordon: "3D femtosecond laser patterning of collagen for directed cell attachment", Biomat. 26, (2005) 4597–4605.
37. J.O. Bonse: „Materialbearbeitung von Halbleitern und Nitridkeramiken mit Ultrakurzen Laserpulsen", PhD, Fakultät II – Mathematik und Naturwissenschaften, Technische Universität Berlin, 2001.
38. www.ubicampus.mh-hannover.de/~bmt/bio/kapitel_6/6_2.php
39. V. Wieger: "Ultra-Short Pulse Laser Ablation of Biological Hard Tissue and Dental Restorative Material", PhD Thesis, Vienna University of Technology, Feb. 2007. Partially published by V. Wieger et al., Proc. Photonics West 2007, PW07L-LAB-21
40. T. Stehrer: "Laser-Induced Breakdown Spectroscopy with the Use of Fibres. Diploma Thesis, Institute of Applied Physics, Johannes-Kepler-Universität, Linz, 2005.
41. M. Capitelli, A. Casavola, G. Colonna, A. de Giacomo: "Laser-Induced Plasma Expansion: Theoretical and Experimental Aspects", Spectrochim. Acta B 59, (2004) 271-289.
42. http://physics.nist.gov

(Received: April 24, 2007, Accepted: December 7, 2007)